Disponible en **www.hormigonyacero.com**
Hormigón y Acero 2023; 74(301):7-20
https://doi.org/10.33586/hya.2023.3120

Influence of Track Typology on the Dynamic Response of Short-Span High-Speed Railway Bridges

Influencia del tipo de vía en la respuesta dinámica de puentes cortos para ferrocarril de alta velocidad

Elena Pilar Martínez[a,b], Gonzalo S.D. Ulzurrun[b], Carlos Zanuy[*,b]

[a] *MC2 Estudio de Ingeniería, Madrid, Spain*

[a] *Department of Continuum Mechanics and Structures, ETS Ingenieros de Caminos, Canales y Puertos, Universidad Politécnica de Madrid, Madrid, Spain*

Recibido el 23 de diciembre de 2022; revisado el 17 de marzo de 2023; aceptado el 25 de abril de 2023

ABSTRACT

It is known that short-span high-speed railway viaducts are prone to suffer significant dynamic effects due to the passage of moving train loads. Recent technological advances in railway engineering have resulted in track typologies different from the conventional ballasted track consisting of discrete sleepers fastened to the rails and resting on a ballast bed. In particular, ballastless track has been identified as an effective solution due to reduced maintenance costs, high track stability and excellent geometric quality. Though different track typologies are available in the market, they can be classified as monolithic or independent according to the interaction degree with the bridge girder. In the present paper, the dynamic behaviour of short-span bridges is numerically studied by taking into account the track-bridge interaction by modelling explicitly the components of the track. Two types of ballastless track (monolithic continuous slab and independent short slabs) and conventional ballasted track are considered on simply supported bridges with span length in the range of 15-25 m subjected to envelope and commercial train loads at speeds between 200 and 360 km/h. In total, 2448 numerical cases have been analyzed. The study shows that dynamic deflections and accelerations produced at the bridge girder by moving train loads can be reduced when the ballasted track is replaced to ballastless track systems, especially for the critical speeds higher than 300 km/h. Moreover, it is shown that the two ballastless track systems lead to very similar results, with the monolithic system resulting in slightly smaller bridge deflections and also moderately larger accelerations.

KEYWORDS: Dynamics; high-speed railway bridges; train loads; ballasted track; ballastless track.

RESUMEN

Es bien conocido que los viaductos para ferrocarril de alta velocidad de luces cortas pueden sufrir importantes efectos dinámicos debido al paso de las cargas de los trenes. Los continuos avances tecnológicos en el ámbito de la ingeniería ferroviaria han dado lugar a nuevos tipos de vía distintos de la tradicional vía sobre balasto formada por una capa de balasto sobre la que descansan las traviesas que van unidas a los carriles. En particular, nuevos diseños de vía en placa sin balasto han surgido como una solución eficaz con bajos costes de mantenimiento, gran estabilidad y excelente calidad geométrica. Aunque existen diferentes tipos de vía en placa, se pueden clasificar en función de su grado de interacción con la estructura del puente, desde monolíticos a independientes. En el presente artículo, se estudia numéricamente la respuesta dinámica de puentes cortos teniendo en cuenta la interacción vía-puente para distintos tipos de vía, incluyendo explícitamente los componentes de la vía en los modelos. Se han considerado dos tipos de vía en placa (monolíticamente unida al tablero del puente o independiente de éste), así como una vía en balasto convencional, en puentes isostáticos de luces cortas en el rango de 15-25 m, sometidos a las acciones ferroviarias de puentes de alta velocidad, incluyendo los trenes envolventes de la normativa y trenes comerciales, con velocidades de circulación entre 200 y 360 km/h, en pasos de 10 km/h. En total, se han resuelto 2448 casos numéricos. El estudio muestra que las flechas y aceleraciones producidas en el tablero por las cargas móviles se pueden reducir cuando se sustituye la vía en balasto por sistemas de vía en placa, especialmente para velocidades superiores a 300 km/h. Además, se ha obtenido que los dos sistemas extremos de vía en placa analizados dan resultados bastante análogos, siendo el sistema monolítico el que resulta en flechas algo menores y aceleraciones algo mayores.

PALABRAS CLAVE: Dinámica, puentes de ferrocarril, interacción puente-vía, alta velocidad, vía en balasto, vía en placa.

* Persona de contacto / *Corresponding author*:
Correo-e / *e-mail*: carlos.zanuy@upm.es (Carlos Zanuy)

How to cite this article: Martínez, E.P., Ulzurrun, G.S.D., Zanuy, C. (2023) Influence of Track Typology on the Dynamic Response of Short-Span High-Speed Railway Bridges, Hormigón y Acero, 74(301):7-20. https://doi.org/10.33586/hya.2023.3120

NOTATION

A	area
C	damping factor
E	modulus of elasticity
I	inertia
K	vertical stiffness
L	span length
M	mass
V	train running velocity
V_{cr}	critical resonant train velocity
a	acceleration at the bridge girder
a_r	acceleration at the rails
b	cross-section width
c	bedding modulus
h	height
f_0	first natural frequency
l	axle load separation
v	vertical displacement at the bridge girder
v_r	vertical displacement at the rails
y_G	distance of the centroid from the bottom of the section
ν	Poisson's ratio
φ'	dynamic amplification factor
φ''	dynamic amplification factor due to irregularities
ρ	density

ACRONYMS

HS	high speed
HSLM	high-speed load model
MSS	mass-spring system
UPM	Universidad Politécnica de Madrid (Technical University of Madrid)

1. INTRODUCTION

A significant growth of the high-speed (HS) railway network has been realized in Europe and Asia for the last decades and further expansion worldwide is expected for the coming years [1]. Reasons for that are the reduction of travel times, better interoperability, and eco-friendliness of railway transport against road transport [2-4]. When referring to HS lines, the commercial speed is typically higher than 200 km/h, which has been proven to produce appreciable dynamic effects on bridges, thus raising concerns of eventual resonance [5-9]. Therefore, structural design codes for HS viaducts have established that dynamic analysis must be performed at the design stage in order to ensure structural safety and users' comfort [10,11]. In terms of structural verifications, a HS bridge design is considered valid in terms of serviceability if accelerations and deformations caused by moving train loads are within specified limits. Accumulated design experience in Spain and other European countries [5,12] has shown that short-span bridges (span length of 25 m or less) are prone to suffer dynamic effects induced by the moving vertical train loads, which are configured as sequences of axle loads passing at the train speed over the structure [10,11]. Accordingly, if the coupled effect of the axle separation and the train speed approaches the natural frequency of the structure, dynamic amplification of the bridge response can be expected.

The continuous technological development in the field of railway track has led to track typologies different from the traditional ballasted track, which consists of a set of discrete rail supports fastened to concrete sleepers which in turn lie on a ballast bed [13]. Ballastless track systems have emerged as an alternative to ballasted track, by substituting the ballast bed and the sleepers by a pavement on which the rails are fastened. Though many types of ballastless track have emerged in the last years [13-15], their general advantages over ballasted track are the better geometric control, smoothness, larger stability, and less maintenance cost, while the higher initial cost has been typically reported as the main disadvantage [2]. For the last years, ballastless track designs have been widely installed in urban areas, metros or tunnels in Europe, while ballasted track is still majority in European mainline tracks [1]. In China and Japan, a significant percentage of the HS network is of ballastless track [1].

Regarding the typologies of ballastless track, they can be classified for the present study according to the interaction degree with the supporting structure: from monolithic to independent systems. In the former, the pavement (typically a continuous concrete slab) is connected to the lower layers so that they work as a composite structure. In the later, an intermediate resilient element is placed between the pavement (floating slab) and the supporting structure. Floating slab systems have been recognized as good solutions for reduction of vibration transmission from the track to the substructure (also referred to as mass-spring systems, MSS [16]) or for mechanical isolation of the track and the substructure when the later has appreciable flexibility (high embankments or flexible bridges).

Connections in fully- or partially-monolithic ballastless track systems can be achieved by an appropriate interface roughness or by connecting dowels. It must be noted that the interaction degree refers here to the response against vertical loads (i.e. the vertical load distribution and contribution to the bending stiffness of the bridge), while further devices can be required to transfer horizontal (longitudinal and transverse) forces (e.g. stoppers, dowels, lateral walls). Examples of monolithic ballastless track designs are the German Rheda [17] and the Spanish BX-AFTRAV [18], in which twin-block concrete sleepers are embedded in a continuous concrete slab poured on site. Independent ballastless track systems can be either continuous (by introducing an intermediate resilient layer below the continuous slab) or short (typically precast) slabs with a thin elastomeric (also referred to as resilient) layer attached on the bottom side. Design examples are the Japanese Shinkansen [19], the Austrian Pörr [20], the Spanish VP-AFTRAV [21] or the Chinese CRTS III [22].

In Spain, ballastless track has been employed in HS mainlines since 2005, with a trend to install on-site solutions of continuous concrete slab with embedded twin-block sleepers in tunnels, embankments in regions with complex orography and stations, and precast solutions on viaducts. Such a trend has been confirmed in 2020-2021 with the installation of precast prestressed concrete slabs of the VP-AFTRAV system on the viaducts of the northern section of the Madrid-Galicia HS line and the new Pajares Pass [23] (Figure 1). It has to be noted

Figure 1. Aerial view of the Tuela Viaduct (Pedralba-Campobecerros section of the Madrid-Galicia HS line, Spain). Precast slabs of VP-AFTRAV ballastless track system. Courtesy by PRECON and Ferrovial.

that such sections are characterized by a difficult layout along mountainous regions, in which the track lies on a sequence of tunnels and viaducts. The track solution consisted of continuous slab track (BX-AFTRAV) in the tunnels and short floating slabs (VP-AFTRAV) on the bridges. The bridge typologies included both single- and multi-span bridges, with span lengths in the range of 20-66 m (mostly within 35-55 m). Twin single-track bridges were dominant instead of double-track bridges due to security reasons imposed by the tunnel-viaduct-tunnel layout.

Even though a dynamic analysis must be done for each particular HS-bridge design according to current standards, the trend to develop new ballastless track systems makes it convenient to analyze the eventual differences of the dynamic response of HS bridges with either track type. It must be remarked that design standards for ballastless track systems are scarce (the European standard [24,25] is rather new, and an ISO group on the subject has just been established) and specific provisions regarding the dynamic track-bridge interaction are not dealt with.

In the present paper, the dynamic response of short-span railway bridges under moving HS train loads is numerically studied. As there is a need to analyze the influence of the track typology, two extreme ballastless track systems (with monolithic and independent interaction with the bridge structure) are compared with conventional ballasted track. The track-bridge interaction is explicitly modeled by including all the components and layers of the track, from the rails to the bridge structure, with the corresponding dynamic properties. It is found that the use of ballastless track systems in short span-bridges is beneficial for the bridge's dynamic behavior as it can reduce the vertical displacements and accelerations produced in the girder by the train loads with respect to those obtained with ballasted track. Thus, the present study will serve as an incentive for engineers to consider ballastless track as an efficient alternative for HS bridges in which the serviceability and comfort limits imposed by design standards might be critical with conventional ballasted track.

2. STUDIED CASES AND SCOPE

The present study is focused on the influence of the track type on the dynamic behavior of short-span HS railway bridges. Statically determinate bridges with a span length between 15-25 m are considered, with three track typologies: conventional ballasted track, continuous slab track monolithically connected to the bridge structure, and short slabs isolated from the bridge structure with an intermediate resilient layer. Hereafter, the later track types will be referred to as monolithic and independent ballastless track systems, respectively. A previous study by the authors [26] has shown that statically determinate bridges present a higher sensitivity to dynamic effects than multi-span statically indeterminate bridges. The later is in agreement with other studies [5,12] and is due to the beneficial mobilization of a higher number of vibration modes in multi-span bridges when train loads act simultaneously in the different spans, while single-span bridges tend to respond mainly with the first vibration mode.

In order to model the bridge, the mechanical properties of the girder (height, area, inertia, centroid position) are necessary. Analytical equations for such properties have been derived as a function of the span length from regression of the particular data extracted from existing HS bridges in Spain. For the regression, the bridges of the northern section of the Madrid-Galicia line and the new Pajares Pass have been taken into account, as they have been the first set of bridges on which ballastless track has been installed in Spain. Nevertheless, such bridges do not present any special differences with bridges with ballasted track, as most of them were initially designed for ballasted track and the track design was modified after the bridge structure had been constructed. A particular aspect of such bridges is that they are single-track structures (Figure 1), which implies that the present study is focused on the flexural behavior without consideration of torsion effects. Future studies will be extended to include torsion. In Figure 2, the regression curves for the mechanical properties of bridge

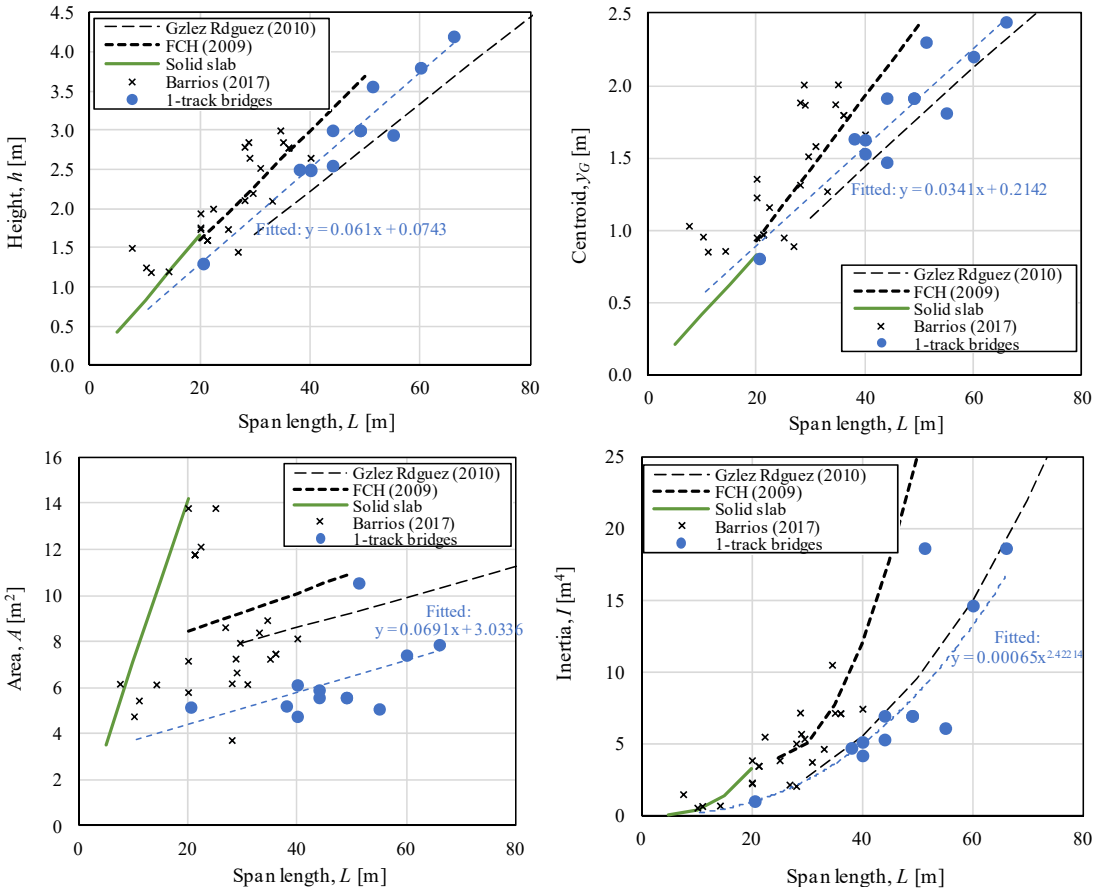

Figure 2. Mechanical properties of HS bridges as a function of the span length.

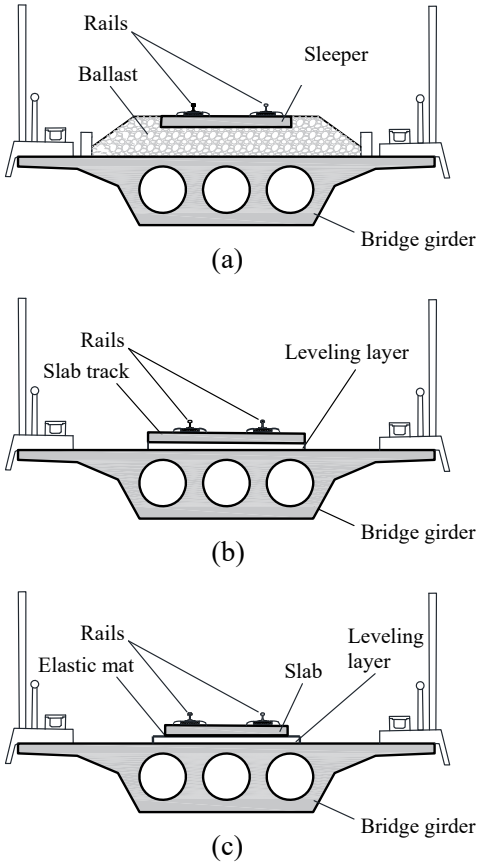

Figure 3. Cross-section of studied track types: (a) Ballasted track; (b) Monolithic continuous slab; (c) Independent short slabs.

girders are obtained by least square fitting as a function of the span length [26]. Blue points represent the real single-track bridges and blue curves are the fitted regression curves, as follows (units in m):

$$h = 0.061L + 0.074 \quad (1)$$

$$y_G = 0.034L + 0.214 \quad (2)$$

$$A = 0.062L + 3.034 \quad (3)$$

$$I = 0.00065L^{2.42} \quad (4)$$

In addition, the mechanical properties of double-track HS bridges have been also plotted in Figure 2 in order to verify the consistency with the previous equations: cross points in Figure 2 refer to the single-span bridges of the HS line Madrid-Zaragoza-Lérida (taken from [27]). Regression lines proposed by [28,29] for double-track Spanish HS bridges are also represented. It can be noted that, in general, mechanical properties of double-track bridges are larger than those of single-track bridges in consistency with the standard width of the cross-section of both cases (14.0 m and 8.5 m, respectively): similar height and centroid depth, but approximately double area and inertia. Lastly, it must be mentioned that the previous regression models are mainly based on bridges with box or hollow-slab cross-sections. As the span length gets shorter, solid slab cross-sections can be also representative, as it can be clearly observed in the larger cross-section area of some cases plotted in Figure 2 than the proposed regression lines. In order to include in the analysis the influence of such a heavier cross-section, a solid slab cross-section (8.5 m width and h/L = 1/12 slenderness) has been also considered for the shortest studied span length (L = 15 m).

The cross-sections of the three considered track types are sketched in Figure 3: a reference conventional ballasted track and two ballastless track systems (monolithic and independent from the bridge girder). The position of the track is considered to be centered with the same vertical axis as the girder, which is consistent with single-track bridge designs and implies no torsion effects (it has to be noted that torsional effects can also exist in single-track bridges with cant, nonsymmetrical position of the track or ballasted track shifting). The conventional ballasted track (Figure 3a) consists of a 0.5 m thick and 5.4 m width ballast layer which supports the monoblock concrete sleepers, which are prisms of 2.6 x 0.22 x 0.25 m3. The longitudinal sleeper spacing is 0.6 m. The rails (UIC60) are joined to the sleepers through fastenings with resilient pad (the mechanical properties of the track components are detailed in Section 3). The monolithic ballastless track system (Figure 3b) consists of a continuous reinforced concrete slab track (3.2 x 0.2 m^2) monolithically joined to the bridge girder with an intermediate leveling layer (0.15 m thick). The leveling layer is assumed here to be of reinforced concrete, but for tracks on embankment it typically consists of a mortar, cement/asphalt or cement-based layer. The interlayer and track-girder connection can be achieved by means of surface roughness in combination with shear keys, dowels or stoppers. Last, the independent ballastless track system (Figure 3c) includes short (5.0 m long) structural concrete slabs (2.5 x 0.2 m² cross-section), supported on a intermediate resilient layer (2 cm thick) which isolates the slabs and the leveling layer (0.15 m thick and 3.0 m width). In both ballastless track systems, rail seat supports are considered at a longitudinal spacing of 0.65 m, with appropriate fastenings (refer to Section 3) between the rails (UIC60) and the slab track.

Particular design details such as the connection systems or the material composition of the track layers are not within the scope of the present paper, due to the huge number of commercial systems and because the attention is paid here at the track-bridge interaction degree since the mechanical viewpoint. Realistic mechanical properties are assumed for the different components (refer to Section 3), so that real commercial systems fall within the two "extreme" cases studied in the present paper. Nevertheless, it can be noted that the monolithic system is characteristic of on-site-built slab-track systems (e.g. Rheda or BX-AFTRAV without under-slab elastic mat) and the independent system is a limit case of floating slab systems (e.g. VP-AFTRAV).

The study presented here is focused on the dynamic effects of vertical train loads considering the track-bridge interaction. In order to capture the dynamic performance and eventual resonance, design codes [10,11] provide the train configuration (axle loads and distances) of a set of commercial and envelope trains. The later, referred to as High-Speed Load Models (HSLM) are assumed to provide the worst envelope from the dynamic viewpoint. Therefore, in the present paper, HSLM-A trains have been considered in the study, in addition to two reference commercial trains (AVE-S101and Talgo-S102) of Spanish HS lines. Train speeds of 200-360 km/h have been analyzed.

3. NUMERICAL METHODOLOGY

The finite element model (FEM) has been employed for the numerical analysis. 2-D models consisting of beams, bars and spring-damper elements have been implemented to reproduce the studied cases. An overview of the FEM schemes is represented in Figure 4. ANSYS v20 [30] software has been used for the solution of the numerical problem, making use of APDL programming language without predefined subroutines. The models include the track-bridge interaction by modeling explicitly the components of the track. Besides the bridge length, 50 m sections of the track on embankment have been also modeled at both sides of the bridge in order to avoid any distortion when the loads enter or leave the bridge (Figure 4). The rails (2 UIC60 rails, see properties in Table 1-Table 3) and the bridge girder are modeled with 2-node Euler beams (BEAM3 in ANSYS), centered in their corresponding centroids. The mechanical properties of the girder are calculated as a function of the span length as detailed in Section 2. The density of the girder is modified with respect to that of structural concrete in order to include the mass of side barriers, handrails, cable conducts, catenaries and ballast retainers (the later only for ballasted track). The beam elements of the rail, ballastless track slab and bridge girder have all the same length, with two elements per fastening spacing.

The model with ballasted track is schematized in Figure 4a. The fastenings are modeled with 2-node vertical spring-damper elements (COMBIN14) of negligible mass,

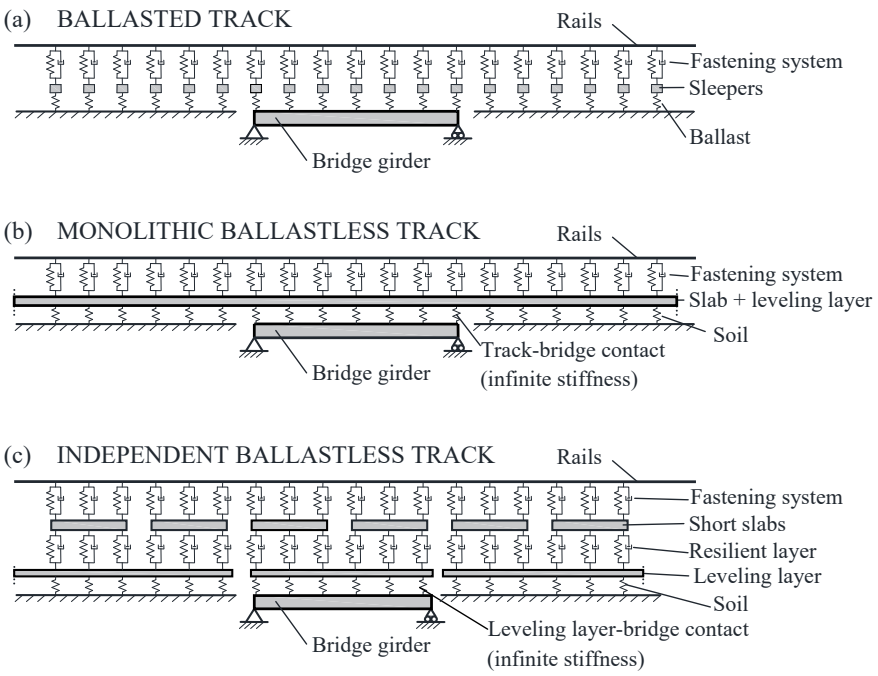

Figure 4. Sketch of finite element models used in the numerical analysis (note that for simplicity of the figure, the horizontal springs of the models have not been plotted in the schemes): (a) Ballasted track; (b) Monolithic continuous slab; (c) Independent short slabs.

with the vertical stiffness and damping coefficient common in Spanish HS lines ([29], refer to Table 1). Then, the sleepers are introduced as single-node concentrated mass elements (MASS21) and, subsequently, the ballast layer is modeled by 2-node vertical springs (LINK1) between the sleepers and the bridge girder. The springs' cross-section area corresponds to the bottom surface of the sleepers and the stiffness is defined in agreement with the normal bedding modulus in Spanish HS lines (0.2 N/mm³, Table 1). The density of the ballast spring elements is set to include the total mass of the ballast layer. Damping of the ballast and the bridge girder is included by Rayleigh beta factors. All mechanical properties of the track components are given in Table 1, in agreement with values of Spanish HS lines.

The monolithic ballastless track is modeled as represented in Figure 4b. Vertical 2-node spring-damper elements are used for the fastening system in a similar way as in the ballasted track, but with corresponding mechanical properties as shown in Table 2 (note that fastenings for ballastless track are commonly more flexible than those for ballasted track). The continuous slab and the leveling layer are modeled as a unique line of Euler beam elements (BEAM3) with the total bending stiffness of both layers (consistent with their monolithic behavior), placed along the slab track's centroid. The connection of the slab track with the bridge girder is achieved with horizontal and vertical spring elements with infinite stiffness so that no relative displacements between the slab and the girder can develop. Note that for simplicity of Figure 4b, the horizontal springs have not been plotted in the schemes.

The model with the independent ballastless track system is plotted in Figure 4c. Mechanical properties of the track components are listed in Table 3. The fastenings between the rails and the slab track are the same as those for the monolithic ballastless track. The short slabs are modeled as Euler beam elements, discontinuous between two adjacent slabs (i.e. every 5.0 m), with a free separation of 0.10 m between slabs. Moreover, the length of the slabs on the bridge edges is shortened so that the joints between the girder and the abutments match with the joints of the slabs at the bridge ends. The leveling layer (continuous Euler beam elements) is rigidly joined to the bridge girder with infinite-stiffness vertical and horizontal springs. The continuity of the leveling layer is interrupted at the bridge ends (refer to Figure 4c). Between the slabs and the leveling layer, 2-node vertical spring-damper elements (COMBIN14) are introduced to reproduce the isolation between the slabs and the bridge achieved with the resilient element. A low vertical stiffness (bedding modulus of 0.015 N/mm³) and a high damping ratio (15%) have been used for the COMBIN14, which correspond to a very flexible elastic material common for ballastless track systems applied to acoustic and vibration mitigation. Typical elastic layers for floating slab systems not requiring vibration reduction capabilities (e.g. VP-AFTRAV) are less flexible (bedding modulus of 0.04-0.2 N/mm³). Thus, the results of the present study correspond to two extreme (but realistic) cases within which most floating slab systems can fall. It has to be noted that for floating slab systems with stiffer intermediate layer, additional horizontal springs might be necessary to consider the eventual tangential interaction between the slabs and the bridge girder.

In the models with ballastless track, vertical spring elements are placed below the leveling layer at the lateral embankment zones, with a bedding modulus of 0.11 N/mm³, which according to the Zimmermann's model [31] corresponds to a modulus of deformation in the loading plate test of E_{v2} = 120 MPa (typically required for ballastless applications [25]). In the models, the boundary conditions at the bridge girder ends are defined to provide simple support (i.e.

the vertical displacements of both supports and the horizontal displacement of one support are constrained, with free rotations).

The dynamic equation of motion of the problem can be summarized as

$$\mathbf{M}\cdot\ddot{\mathbf{x}}(t) + \mathbf{C}\cdot\dot{\mathbf{x}}(t) + \mathbf{K}\cdot\mathbf{x}(t) = \mathbf{F}(t) \quad (5)$$

where **M**, **C** and **K** are the global mass, damping and stiffness matrices built with the above explained parameters, $\mathbf{x}(t)$ contains the nodal displacements vector, and $\mathbf{F}(t)$ is the vector with time-variable nodal forces. Train loads are introduced as a set of moving loads by distributing the corresponding axle loads in each node as a function of time, which in turn depends on the train velocity. Explicit vehicle-track interaction is not within the scope of the paper due to the difficulties to determine mechanical properties of the vehicles [7] and because design criteria require the calculation of the effects produced by envelope HSLM trains described only by axle loads. For such HSLM trains, mass distribution, damping properties and sub-component stiffness are not defined. Nevertheless, it has been reported that dynamic analysis without explicit vehicle-track interaction are on the safe side with respect to those including such an interaction [32][33]. The role played by the different components of train-track-bridge interaction models has been comprehensively discussed by Zhai et al. [34]. An alternative way to include the effects of such an interaction might be the introduction of an increased damping factor to the structure [11]. Herein, the vertical load distributions are taken according to the HSLM-A trains, as well as to two commercial trains (AVE-S101 and Talgo-S102) characteristic of Spanish HS lines [10,11], with running speeds in the range of 200-360 km/h with a step size of 10 km/h. For both HSLM and commercial trains, the axle load configuration defined in Annex C.2 of IAPF [10] has been used in the numerical analysis.

For the solution of the dynamic problem (Eq. (5)), transient analysis with full-time integration has been used. Modal superposition analysis has not been carried out in order to capture all relevant vibration modes including those of the track, without a-priori low-pass frequency limitation and to avoid the controversy of pre-selecting the excited modes [35]. For the numerical solution, the Newmark integration procedure [36] with default ANSYS parameters (γ = 0.005, α = 0.2525, δ = 0.5050) has been used, which is unconditionally stable [37]. A variable time step has been employed, with a normal, minimum and maximum value of 0.001, 0.0003 and 0.01 s. The average computational time for each case has been 5 min.

4. ANALYSIS OF RESULTS

4.1. Identification of natural frequencies

Before the transient analysis of the dynamic response produced by train loads, a first identification of natural frequencies and vibration modes has been carried out by means of modal extraction and harmonic analysis. It has to be noted that due to the track-bridge interaction model, several vibration modes can be obtained from a conventional modal extraction analysis due to excitation of the track components. Therefore, a harmonic analysis has been performed consisting of a simulation of the model's response to a sinusoidally repeating dynamic load of amplitude 100 kN and frequency range from 0.1 to 200 Hz, applied at a node of the rails placed eccentrically with respect to the bridge midspan to allow for excitation of both symmetric and asymmetric vibration modes. The peak-picking identification of the response's magnitude allows for determining the relevant natural frequencies (refer to Figure 5). The natural frequencies of the first 4 vibration modes of the bridge are compared in Figure 6. The average first natural frequency of the model for the three track types, which is the mainly excited one in simply supported bridges, is 7.7 Hz (L = 15 m), 5.8 Hz (L = 20 m) and 4.6 Hz (L = 25 m). Moreover, Figure 6 shows that the smallest natural frequencies are found for the models with ballasted track and the highest for those with monolithic ballastless track, which is due to smaller mass (no ballast layer) of the later and the contribution of the slab track to the bending stiffness of the bridge. The natural frequencies of the models with independent ballastless track system are in-between, due to the smaller contribution of the isolated short slabs to the bending stiffness.

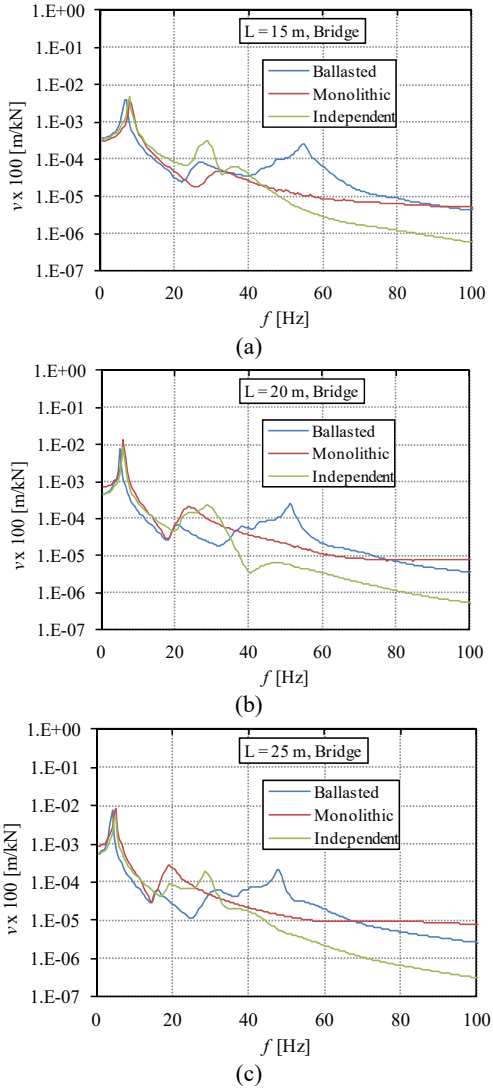

Figure 5. Magnitude of the bridge harmonic response in the 0-100 Hz frequency range (a) L = 15 m; (b) L = 20 m; (c) L = 25 m.

4.2. *Time-dependent results*

Detailed time-dependent results of all numerical cases have been extracted in terms of the vertical deflection and acceleration at the midspan, both at the bridge girder and at the rails. In general, considered train loads consist of one or two subsequent compositions of two locomotives (front and rear) and a number of carriages in-between. The highest structural effect is in many cases governed by the locomotives, as they have more axles at a closer distance to each other than the carriages. Nevertheless, when the relationship between the axle distance of the carriages and the running speed is such that the excitation frequency approaches the natural frequency of the structure, a higher dynamic amplification of the structural response is obtained. Eventual resonance takes place when both frequencies are equal, though damping components modulate the dynamic amplification. Given the first natural frequency of the structure (f_0), a theoretically critical speed (V_{cr}) of each set of train loads can be estimated as a function of the dominant load separation (l), as follows [38]:

$$V_{cr} = l \cdot f_0 \tag{6}$$

According to the first natural frequencies obtained in Section 4.1, the critical speeds of HSLM-A trains should fall between 257-693 km/h, since the carriages sequence of such trains is characterized by sets of 2 equal loads spaced at distances in the range of 15.5-25 m between their centers. In the case of the Talgo-S102 train, the carriages sequence is defined by single 170 kN loads spaced at 13.14 m (V_{cr} = 216-364 km/h), while the AVE-S101 has sets of 2 axle loads with a spacing of 18.7 m between their centers (V_{cr} = 310-518 km/h). It has to be noted that the previous values of V_{cr} are based on the average first natural frequency of the three track types. Exact values of V_{cr} for each track type can vary from them according to the particular track-bridge details and train sequence.

In order to exemplarily show the dynamic response of studied cases, the time histories of vertical displacements and accelerations at midspan are depicted in Figure 7-Figure 9 regarding the response of the 20 m span bridge produced by the Talgo-S102 running at the critical velocity corresponding to the three track types: ballasted track (V_{cr} = 246 km/h), monolithic (V_{cr} = 291 km/h) and independent (V_{cr} = 285 km/h) ballastless track systems. In order to assess the beneficial effect of damping on the dynamic amplification, the numerical cases have been simulated with and without damping. The influence of damping can be clearly observed through the smaller displacements and accelerations of models with damping than without damping, but especially visible is the result of the midspan deflection at the bridge girder (v in the graphs of Figure 7-Figure 9). For instance, if the model with ballasted track is considered (Figure 7), the results without damping show a clear amplification of the midspan displacement (v) produced by the subsequent actuation of the axle loads of the carriages (see intervals of 1.5-3.0 s and 4.0-5.5 s in Figure 7). The dynamic displacement of the carriages obtained in the model without damping is around 2 times that of the model with damping. Nevertheless, the resonance of the carriages of the Talgo-S102 is not the worst effect, because the highest displacement is the one produced by the locomotives' axles (time intervals of 0.6-1.5 s, 3.0-4.0 s and 5.5-6.0 s in the bridge with ballasted track, see Figure 7). Similar conclusions can be reached by observing the midspan displacement and acceleration at the bridge girder with the three track types.

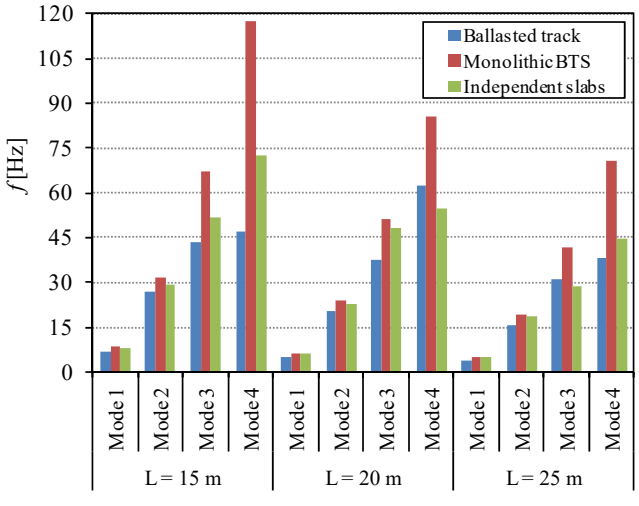

Figure 6. Natural frequencies of the first 4 vibration modes.

Additional differences are found regarding the dynamic response at the rails (v_r and ar in Figure 7 - Figure 9), as the isolation between the track and the bridge in the model with independent ballastless track results in appreciably higher rail displacements (v_r) and accelerations (a_r) than the other track types. However, the beneficial effect of the damping components can be also observed in such a case (Figure 9).

4.3. *Derivation of envelopes*

The time-history analysis explained in the previous Section has been carried out for all studied cases and the maximum values of midspan displacements and accelerations have been collected as a function of the train type and the running speed for each bridge configuration (span length and track type). As an example, such maxima at the bridge girder have been represented in Figure 10 for a span length of L = 20 m. It can be observed that each train produces the highest excitation at different velocities, which is a function of the coupling of the axles' configuration and the running speed with the natural frequency of the structure, as discussed in Section 4.2. From Figure 10, it can be observed that significant dynamic effects are obtained in the 20 m span bridge with ballasted track for train speeds higher than 300 km/h, while the displacements and accelerations are significantly smaller if the ballasted track is replaced to ballastless track (either monolithic or independent).

In order to elaborate more on the previous observations for span length of 20 m, envelope curves have been obtained for all simulated cases from the peak results produced by each train. The envelope curves have the ability to provide the worst effects (highest midspan displacement and acceleration), as represented in Figure 11. The analysis has shown that the governing train configurations of the envelope curves are mostly the HSLM-A trains, but in some cases the AVE-S101 has been the critical one (especially for the shortest bridge length), which shows that commercial trains

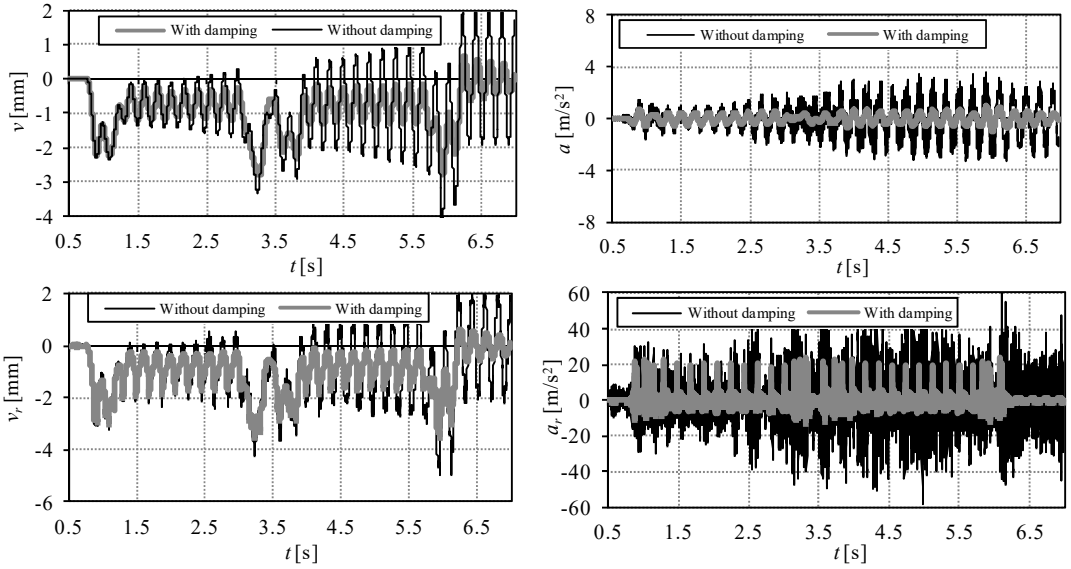

Figure 7. Displacement and acceleration histories at midspan (L = 20 m, ballasted track, Talgo-S102 train, V_{cr} = 246 km/h).

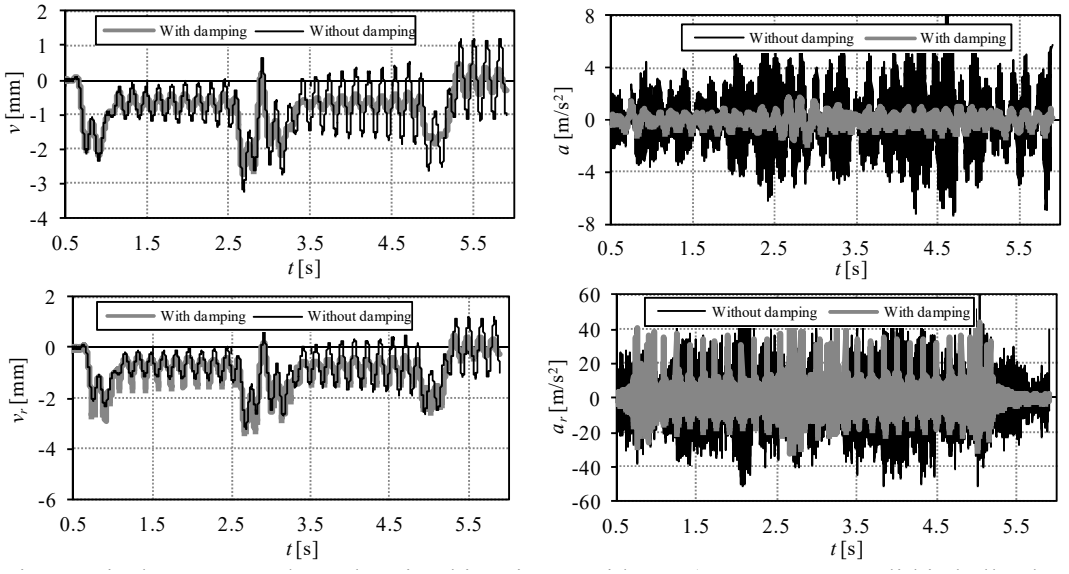

Figure 8. Displacement and acceleration histories at midspan (L = 20 m, monolithic ballastless track, Talgo-S102 train, V_{cr} = 291 km/h).

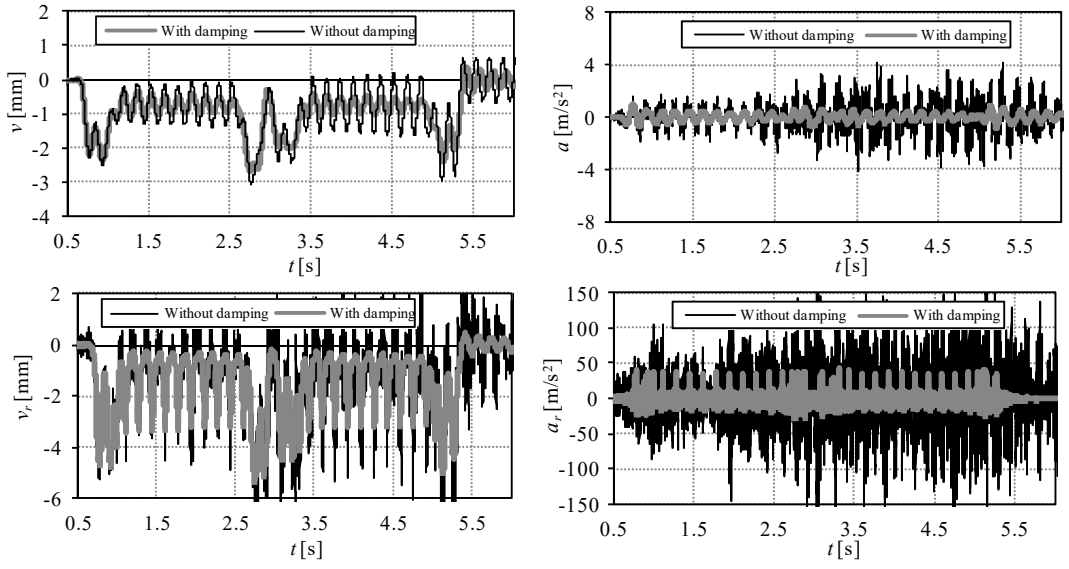

Figure 9. Displacement and acceleration histories at midspan (L = 20 m, independent slabs, Talgo-S102 train, V_{cr} = 285 km/h).

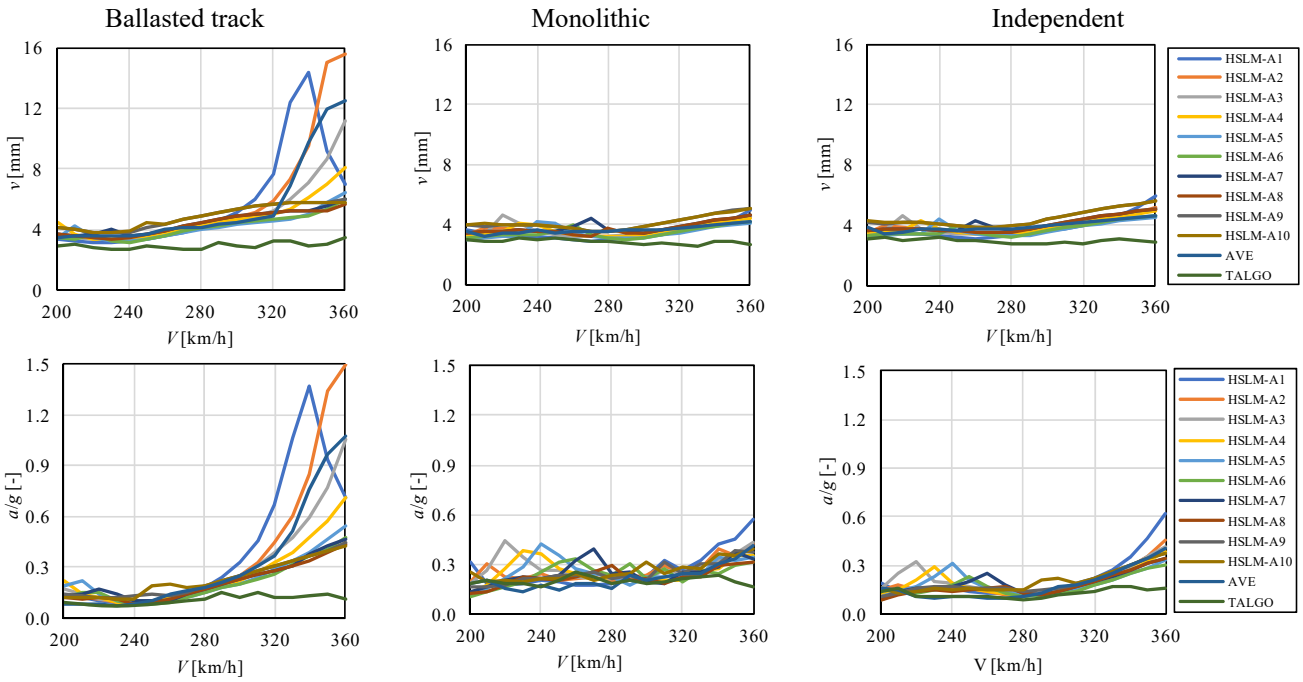

Figure 10. Peak displacements and accelerations at bridge midspan obtained in the simulations with span length L = 20 m.

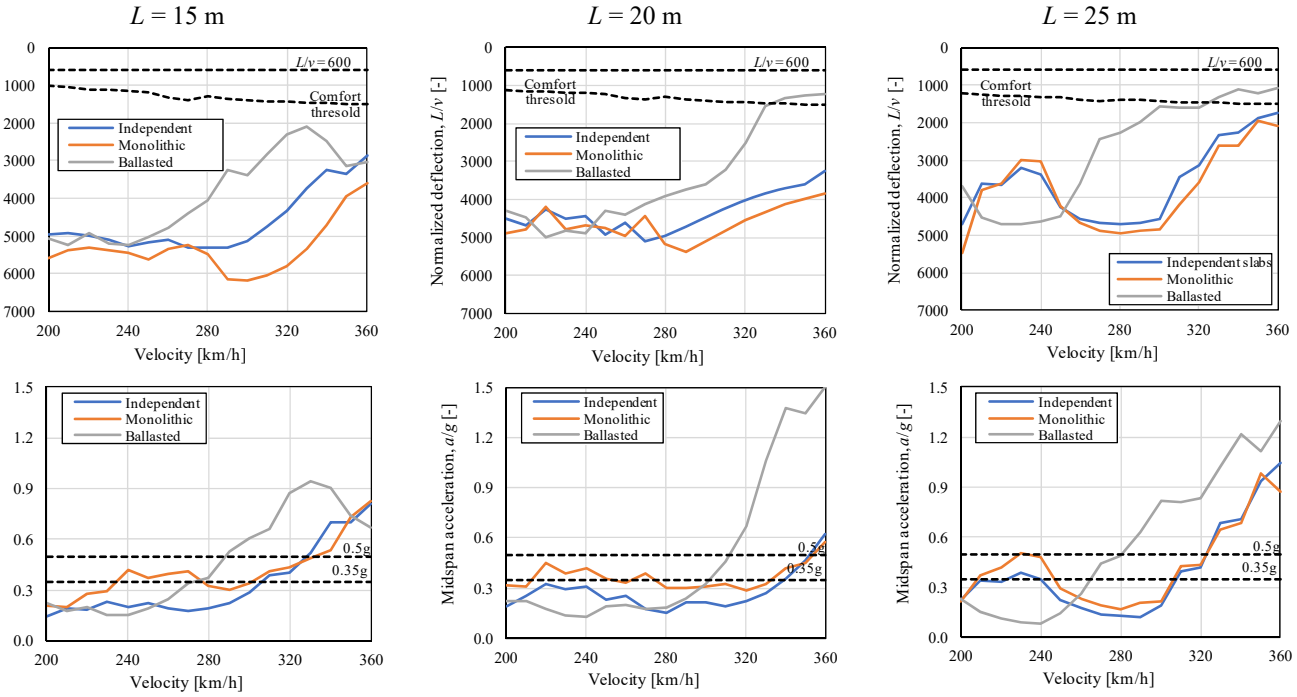

Figure 11. Envelope curves of peak displacements and accelerations at bridge midspan.

might lead to worse dynamic effects than HSLM-A trains in short-span bridges. In the graphs of Figure 11, the midspan deflection has been normalized to the span length (v/L) and the acceleration is normalized to the gravity acceleration (g).

To allow for analyzing serviceability issues including users' comfort, the limitations of design codes [10,11] are included in Figure 11. Such limitations are defined in terms of the maximum vertical acceleration (0.35g and 0.5g for ballasted and ballastless tracks, respectively) and the midspan displacement (L/600), both at the bridge girder. Structural design codes also provide limits for the accelerations in the train in order to ensure the users' comfort. Nevertheless, such accelerations cannot be checked unless explicit train-track interaction is included in the models. Alternatively, the codes [10,11] recommend a more strict limit for the bridge displacement than L/600 as a function of the running speed and span length, which has been also represented in Figure 11. Arvidsson et al. [39] have reported that the acceleration limit for ballastless track could be increased up to 1-3g without compromising infrastructure and running safety.

4.4. *Influence of track type*

In general terms, Figure 11 shows that the highest displacements and accelerations are obtained in the models with ballasted track, which means that the use of ballastless track systems in short-span railway bridges can be helpful to reduce dynamic effects. Regarding the two systems of ballastless track studied, bridge deflections and accelerations are rather similar, but in most of the cases the models with monolithic slab track show smaller deflection and higher acceleration than the models with independent slabs, which is closely related with the contribution of the slab track to the stiffness of the system.

For the shortest span length (L = 15 m in Figure 11), the bridge midspan displacement increases significantly for speeds higher than 250 km/h for the model with ballasted track, while such displacements start to increase appreciably from 300 km/h for ballastless tracks, remaining the later always smaller than those of the model with ballasted track. Similar results are obtained in terms of the peak acceleration, which shows that the discomfort limit (0.35g and 0.5g, depending on the track type) is overcome for speeds higher than 275 km/h with ballasted track and 330 km/h with ballastless tracks.

For the bridge with L = 20 m span length, the girder midspan deflection increases significantly for speeds higher than 300 km/h with the ballasted track, and the comfort threshold is even reached from a speed of 330 km/h. The use of ballastless track results in smaller midspan deflections, which lie always below the comfort threshold. The accelerations at the bridge midspan overcome the comfort limit (0.35g) for speeds higher than 300 km/h in case of ballasted track, while the comfort limit (0.5g) is only reached for speeds higher than 350 km/h with ballastless track systems.

The results of the bridge with span length of L = 25 m are very similar to those with L = 20 m. The comfort threshold for bridge displacements is overcome for speeds higher than 325 km/h with ballasted track but it is never reached with ballastless tracks. Regarding the bridge accelerations, they are higher than the limit of 0.35g for ballasted track for speeds higher than 265 km/h, while the limit of 0.5g for ballastless track is reached from a speed of 320 km/h.

An interesting result for the longest bridge (L = 25 m) is that for moderate velocities (200 < V < 250 km/h, still in the HS range), the dynamic response of the bridge (accelerations and displacements) is larger with ballastless track than with ballasted track, though the comfort and serviceability limits are not reached. Moreover, within ballastless track types, the response within such a speed range is slightly higher with the monolithic slab track than with the independent slabs. Similar trend (but less pronounced) is obtained with the shorter span lengths (15 and 20 m).

4.5. *Influence of bridge cross-section*

The former results have been obtained by considering that the mechanical properties of the bridge girder can be calculated with Eqs. (1)-(4). It has to be noted that such equations (as well as those proposed by [28,29] for double track bridges) have been mainly fitted from girder typologies of box- or hollow-core slab sections. Nevertheless, a detailed observation of Figure 2 shows that many real bridges fall far from the fitted equations for the shorter span lengths, which can be explained by the existence of stiffer cross-section typologies like solid slabs. In order to analyze the influence of the stiffness of the cross-section, the simulations have been repeated with a solid slab with h/L = 1/12 slenderness for the shortest span length (L = 15 m). The corresponding mechanical properties of the bridge girder are represented in Figure 2 with green lines.

The influence of the cross-section type can be analyzed with the comparison of deflections and accelerations at the bridge midspan plotted in Figure 12. In the graphics, the envelopes of dynamic response show a significant reduction of peak deflections and accelerations when the girder consists of a solid slab. Therefore, it can be concluded that another alternative to improve the dynamic performance of short-span bridges can be to increase the size of the cross-section.

4.6. *Results at the rails*

The envelopes of midspan vertical deflections and accelerations obtained at the central node of the rails are represented in Figure 13. As it can be noted, the highest displacements at the rails are obtained either with the ballasted track or with the independent ballastless track system, depending on the span length and the velocity. The smaller displacements obtained with the monolithic ballastless track can be explained by the joined vertical performance of the bridge and

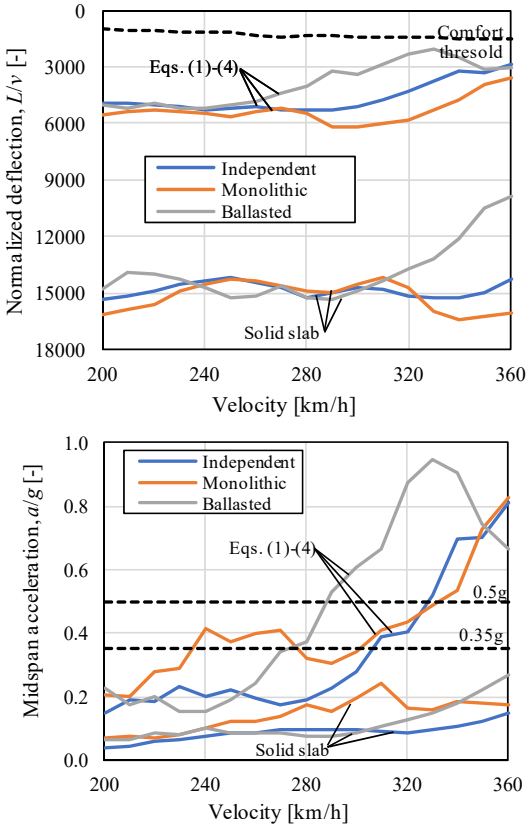

Figure 12. Comparison of dynamic envelopes of bridge midspan deflection and acceleration for span length L = 15 m, with different bridge cross-section.

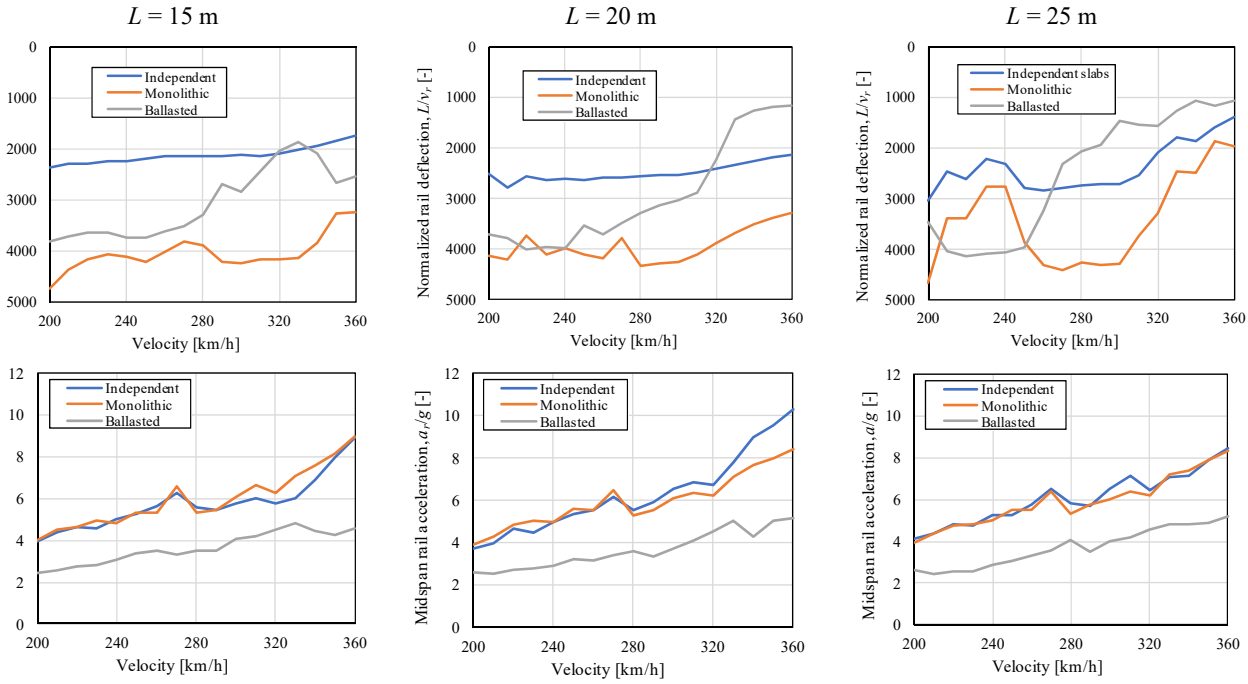

Figure 13. Envelope curves of peak displacements and accelerations at the rails.

the slab track, which means that the rails are only separated from the slab track by the fastenings. In the ballasted track and the independent ballastless track, the rails are further isolated from the bridge by the intermediate elastic layers (ballast bed and resilient elastomeric mat, respectively). Regarding the vertical accelerations, Figure 13 shows that the ballasted track is the system with smallest accelerations in the rails, while the two ballastless track systems show rather similar rail accelerations. Even though rail accelerations may seem high as a result of the track-bridge interaction model subjected to moving loads, they are on the safe side with respect to other models considering explicitly the train suspension and oscillations [33]. Furthermore, the significance of the verification of passengers comfort through criteria based on deflections and accelerations at the bridge girder has been confirmed by authors considering the train-track-bridge interaction [39].

¡An additional aspect that deserves to be discussed when dealing with the track-bridge interaction is the influence of the track irregularities. In the present research, such irregularities have not been taken into account. Nevertheless, the additional dynamic amplification due to track or wheel defects in HS lines is typically small due to the stringent maintenance of such lines. A rough estimation of the effects due to track irregularities and vehicle imperfections can be done with the formulation provided by [10,11], which estates that the total dynamic amplification factor in railway bridges can be expressed as $1 + \varphi' + r \cdot \varphi''$, where φ' is the amplification produced by dynamic loads and $r \cdot \varphi''$ is the additional effect due to irregularities ($r = 0.5$ for HS lines), as follows:

$$\varphi'' = a\left[0.56e^{-\left(\frac{L}{10}\right)^2} + 0.50\left(\frac{f_0 L}{80} - 1\right)e^{-\left(\frac{L}{20}\right)^2}\right], a = \min\left(\frac{V}{22}, 1\right) \quad (7)$$

where V is expressed in m/s.

According to Eq. (7), the highest amplification due to track and vehicle irregularities for the highest speed (360 km/h) would range from 1.3% (L = 25 m, ballasted track) to 11.0% (L = 15 m, monolithic ballastless track). Nevertheless, such values could be refined with more complex vehicle-track-bridge interaction models out of the scope of the present paper.

5. CONCLUSIONS

The present study has focused on the dynamic behavior of short-span HS railway bridges subjected to vertical moving train loads, with special attention at the influence of the track typology. Three track types have been considered, namely conventional ballasted track and two ballastless tracks, with monolithic and independent interaction with the bridge structure. The most relevant conclusions reached in the present study are as follows:

- The track type can play a significant role in the dynamic response of short single-span HS railway bridges subjected to moving train loads. The simulations show that dynamic amplifications suffered by the bridge structure with ballasted track might lead to deflections and accelerations higher than the limits specified by design codes. The introduction of ballastless track systems can reduce significantly the bridge deflections and accelerations, so that the codes' limitations can be fulfilled. In the worst cases, the critical velocity range leading to excessive accelerations is appreciably reduced with respect to ballasted track. Thus, ballastless track systems can be an effective solution to reduce dynamic effects on short-span HS railway bridges.

- The influence of the interaction degree between the ballastless track and the bridge girder is rather limited regarding the effects produced on the bridge girder. The monolithic system leads to slightly smaller bridge deflections and also moderately larger accelerations. It has to be noted that the present paper has mainly focused on the bridge design implications; thus, further consequences of the track-bridge interaction degree for the slab track design are outside the scope of the paper (regarding e.g. the reinforcement detailing required in monolithic systems when the slab accompanies the girder deformation or the bending solicitation of floating slabs).
- Though ballastless track systems generally result in smaller peak deflections and accelerations at the bridge girder than ballasted track, the effects at the non-critical velocity range of 200-260 km/h produced by ballastless track can be larger than those caused by ballasted track.
- For short span bridges, it has been shown that bridge cross-sections consisting of a solid slab provide a better dynamic response, reducing significantly the accelerations and deflections produced by HS train loads with respect to more slender cross-section typologies. Thus, the combination of an appropriate bridge cross-section design and ballastless track system seems to be an interesting approach for the mitigation of dynamic effects caused by HS train loads.
- Dynamic effects (displacements and accelerations) at the rails can have different trends than those at the bridge girder: the simulations show that the highest rail displacements are obtained with independent ballastless track systems and ballasted track, while the largest accelerations are found for the two ballastless track systems. A refined estimation of rail accelerations and deflections could be completed with detailed vehicle models, but the indirect verification of passengers' comfort and running safety through accelerations and displacements at the bridge girder is well established in the standard provisions.
- The numerical simulations have shown that the train configurations leading to the worst dynamic effects are not always the HSLM-A trains. In some cases, the AVE-S101 has been the critical one, especially with the shortest bridge length of 15 m.

Acknowledgements

Interesting insights provided by AFTRAV (Spanish Association for Manufacturers of Sleepers) are gratefully acknowledged. The present paper is based on the models prepared in the Master's thesis of Ref. [26].

TABLE 1.
Mechanical properties of ballasted track [29].

Track component	*Element designation*	*Material properties*	*Mechanical properties*
Rail UIC-60	BEAM3	E = 210 GPa, ν = 0.3, ϱ = 7.85 t/m^3	A = 2x76.7 cm^2, I = 2x3038cm^4, y_G = 8.1 cm; h = 172 mm
Fastening system	COMBIN14		K = 150 kN/mm; C = 15 kNs/m
Sleeper	MASS21	M = 0.36 t	-
Ballast layer	LINK1	ϱ = 1.8 t/m^3	c = 0.2 N/mm^3, C = 12.3 kNs/m/rail seat
Bridge girder	BEAM3	E = 37.1 GPa, ν = 0.2, ϱ = 2.5 t/m^3 (+ mass of non-structural elements)	A, I, h, y_G acc. to span length, ξ = 2%

TABLE 2.
Mechanical properties of monolithic ballastless track [29].

Track component	*Element designation*	*Material properties*	*Mechanical properties*
Rail UIC-60	BEAM3	E = 210 GPa, ν = 0.3, ϱ = 7.85 t/m^3	A = 2x76.7 cm^2, I = 2x3038cm^4, y_G = 8.1 cm; h = 172 mm
Fastening system	COMBIN14		K = 50 kN/mm, C = 15 kNs/m
Slab track and leveling layer	BEAM3	E = 37.1 GPa, ν = 0.2, ϱ = 2.5 t/m^3	Rectangular cross-section of slab and leveling layer
Slab-leveling layer-girder contacts	LINK1	ϱ = 0 t/m^3, E = ∞	Tributary area of one rail seat
Bridge girder	BEAM3	E = 37.1 GPa, ν = 0.2, ϱ = 2.5 t/m^3 (+ mass of non-structural elements)	A, I, h, y_G acc. to span length, ξ = 2%

TABLE 3.
Mechanical properties of independent ballastless track [29].

Track component	*Element designation*	*Material properties*	*Mechanical properties*
Rail UIC-60	BEAM3	E = 210 GPa, n = 0.3, ϱ = 7.85 t/m^3	A = 2x76.7 cm^2, I = 2x3038cm^4, y_G = 8.1 cm; h = 172 mm
Fastening system	COMBIN14		K = 50 kN/mm; C = 15 kNs/m
Slab Track and leveling layer	BEAM3	E = 37.1 GPa, ν = 0.2, ϱ = 2.5 t/m^3	Rectangular cross-section of slab and leveling layer
Slab-leveling layer contact	COMBIN14	c = 0.015 N/mm^3; ξ = 15%	Tributary area of one rail seat
Leveling layer-girder contact	LINK1	ϱ = 0 t/m^3, E = ∞	Tributary area of one rail seat
Bridge girder	BEAM3	E = 37.1 GPa, ν = 0.2, ϱ = 2.5 t/m^3 (+ mass of non-structural elements)	A, I, h, y_G acc. to span length, ξ = 2%

References

[1] UIC. High speed lines in the world. 2021. International Union of Railways, Paris.

[2] UIC. High Speed Rail. Fast track to sustainable mobility. 2018. International Union of Railways, Paris.

[3] Kang, C., Schenider, S., Wenner, M., Marx, S. (2018) Development of design and construction of high-speed railway bridges in Germany. *Engineering Structures* 163:184-196. https://doi.org/10.1016/j.engstruct.2018.02.059

[4] European Commission. High-speed Europe. A sustainable link between citizens. 2010. European Commission, Brussels.

[5] Goicolea, J.M.. (2011) Acciones dinámicas debidas al tráfico ferroviario en viaductos de alta velocidad. *Proceedings of Seminario Torroja 2011*, Madrid, Spain

[6] Goicolea, J.M., Domínguez, J., Gaaldón, F., Navrro, J.A. (2002) Resonant effects in short span high speed railway bridges: modelling and design issues. *Proceedings of the International Conference Eurodyn 2002*, Munich, Germany.

[7] Feng, D., Feng, M.Q. (2015) Model updating of railway bridge using in situ dynamic displacement measurement under trainloads. *Journal of Bridge Engineering* 20:04015019. https://doi.org/10.1061/(ASCE)BE.1943-5592.0000765

[8] Jiang, H., Gao, L. (2020) Analysis of the vibration characteristics of ballastless track on bridges using an energy method. *Applied Sciences* 10:2289. https://doi.org/10.3390/app10072289

[9] Ju, S.H., Lin, H.T. (2003) Resonance characteristics of high-speed trains passing simply supported bridges. *Journal of Sound and Vibration* 267:1127-1141. https://doi.org/10.1016/S0022-460X(02)01463-3

[10] Spanish Ministry for Public Works. (2007) IAPF-07 Spanish code for loads to be considered in the design of railway bridges. Madrid.

[11] CEN. EN 1991-2:2003. Eurocode 1. Actions on structures - Part 2: Traffic loads on bridges. Brussels, Belgium, 2002.

[12] ACHE. Monograph M-15: Application examples of IAPF-07. 2009. Spanish Association for Structural Engineering, Madrid, Spain.

[13] Esveld, C. (2001) Modern railway track. Delft, The Netherlands: Esveld MRT-Productions.

[14] Michas, G. (2012) Slab track systems for high-speed railways; Master's Degree Project. Royal Institute of Technology, Stockholm.

[15] Zhai, W., Wang, K., Chen, Z., Zhu, S., Cai, C., Liu, G. (2020) Full-scale multi-functional test platform for investigating mechanical performance of track-subgrade systems of high-speed railways. *Railway Engineering Science* 28:213-231. https://doi.org/10.1007/s40534-020-00221-y

[16] Tomicic-Torlakovic, M., Budisa, M., Radjen, V. (2012) Slab track mass-spring system. Transportation Research Record: *Journal of the Transportation Research Board* 2289:64-69. https://doi.org/10.3141/2289-09

[17] Freudenstein, S. (2010) Rheda 2000: ballastless track systems for high-speed rail applications. *International Journal of Pavement Engineering* 11:293-300. https://doi.org/10.1080/10298431003749774

[18] ADIF. NAV 7-1-0.7 Diseño y montaje de vía sin balasto para obra nueva (Design and execution of ballastless track for new constructions), Chapter 7.3 Construction of concrete pavement . 2021. Madrid, Spain.

[19] Ando, K., Sunaga, M., Aoki, H., Haga, O. (2001) Development of slab tracks for Hokuriku Shinkansen line. *Quarterly Report of RTRI* ;42:35-41. https://doi.org/10.2219/rtriqr.42.35

[20] Porr Technobau und Umwelt AG. Slab Track Austria. Elastisch gelagerte Gleistragplatte. 2022. Vienna, Austria.

[21] Albajar, L. (2012) La vía sin balasto a partir de placas prefabricadas de AFTRAV (Ballastless track with AFTRAV precast concrete slabs). ANDECE, Madrid, Spain.

[22] Wang, B.Q., Pei, L., Ai, Q.K., Zheng, H.B., Si, W. (2017) Key innovative technology of CRTS III type pre-tensioning ballastless track slab by unit serial method. 2nd International Conference on Intelligent Transportation Engineering (ICITE).103-107. Singapore. https://doi.org/ 10.1109/ICITE.2017.8056890

[23] MAFEX. (2021) VP slab track system. MAFEX Corporate Magazine of the Spanish Railway Association 27:84.

[24] CEN. EN 16432-1: 2018 Ballastless track systems. Part 1: general requirements. 2018. Brussels, Belgium,

[25] CEN. EN 16432-2: 2018 Ballastless track systems. Part 2: system design, subsystems and components. 2018. Brussels, Belgium,

[26] Martínez González, E.P. (2022) Effects of moving loads on railway bridges considering the structure of railway track. Master's thesis, Universidad Politécnica de Madrid, Madrid, Spain.

[27] Barrios Fragoso, E. (2017) Estudio dinámico de puentes de ferrocarril isostáticos y de luces cortas. Línea de alta velocidad Madrid-Barcelona-Frontera francesa. Master's thesis, Universidad Politécnica de Madrid, Madrid, Spain.

[28] González Rodríguez, O. (2010) Interacción vía-estructura en puentes de ferrocarril. Master's thesis, Universidad Politécnica de Madrid, Madrid, Spain.

[29] Goicolea, J.M., Cuadrado, M., Viñolas, J., Galvín, P., Mateos, A. (2012) Estudio del comportamiento a medio y largo plazo de las estructuras ferroviarias de balasto y placa. CEDEX (Spanish Research and Experimentation Center for Public Works), Monograph 111, Madrid, Spain

[30] ANSYS I. Ansys Mechanical v. 20.0 user's guide. Southpointe, 275 Technology Drive, Canonsburg, PA 15317: Ansys, Inc., 2020.

[31] Zimmermann, H. (1888) *Die Berechnung des Eisenbahnoberbaus*. Ernst & Sohn, Berlin, Germany.

[32] Domínguez Barbero, J. (2001) Dinámica de puentes de ferrocarril para alta velocidad: métodos de cálculo y estudio de la resonancia. PhD Thesis, Universidad Politécnica de Madrid, Madrid, Spain.

[33] Museros, P., Romero, M.L., Poy, A., Alarcón, E. (2002) Advances in the analysis of short span railway bridges for high-speed lines. *Computers and Structures* 80:2121-2132. https://doi.org/10.1016/S0045-7949(02)00261-4

[34] Zhai, W., Xia, H., Caía, C., Gaoc, M., Lid, X., Guoe, X., et al. (2013) High-speed train-track-bridge dynamic interactions. Part 1: theoretical model and numerical simulation. *International Journal of Rail Transportation*;1:3-24. https://doi.org/10.1080/23248378.2013.791498

[35] Museros, P., Alarcón, E. (2005) Influence of the second bending mode on the response of high-speed bridges at resonance. *Journal of Structural Engineering* 131:405-415.

[36] Newmark, N.M. (1959) Method of computation for structural dynamics. ASCE *Journal of Engineering Mechanics Division*, 85:67-94.

[37] Hughes, T.J.R. (1987) *The finite element method. Linear static and dynamic finite element analysis*. Englewood Cliffs, NJ: Prentice-Hall.

[38] Ju, S.H., Lin, H.T., Huang, J.Y. (2009) Dominant frequencies of train-induced vibrations. Journal of Sound and Vibration 319:247-259. https://doi.org/10.1016/j.jsv.2008.05.029

[39] Arvidsson, T., Anderss on, A., Karoumi, R. (2019) Train running safety on non-ballasted bridges. International Journal of Rail Transportation, 7:1-22. https://doi.org/10.1080/23248378.2018.1503975